Uluslararası İleri Doğa Bilimleri ve Mühendislik Araştırmaları Dergisi
Sayı 9, S. 37-47, 9, 2025

Araştırma Makalesi

IJANSER
https://as-proceeding.com/index.php/ijanser
ISSN:2980-0811

International Journal of Advanced Natural Sciences and Engineering Researches
Volume 9, pp. 37-47, 9, 2025

Research Article

Simulation of Longitudinal Vehicle Dynamics under FTP-75 Drive Cycle Using MATLAB/Simulink

Serhat Küçükdermenci *

Department of Electrical and Electronics Engineering, Faculty of Engineering, Balikesir University, 10463, Balikesir, Türkiye

**kucukdermenci@balikesir.edu.tr*

(Received: 03 September 2025, Accepted: 07 September2025)

(7th International Conference on Innovative Academic Studies ICIAS 2025, September 02-03, 2025)

ATIF/REFERENCE: Küçükdermenci, S. (2025). Simulation of Longitudinal Vehicle Dynamics under FTP-75 Drive Cycle Using MATLAB/Simulink, *International Journal of Advanced Natural Sciences and Engineering Researches*, 9(9), 37-47.

Abstract **–** This study presents a MATLAB/Simulink-based framework for analyzing the longitudinal dynamics of passenger vehicles under standardized drive cycles. The primary objective is to provide a flexible tool for quantifying tractive effort, power demand, and wheel torque , which are critical for the design and performance evaluation of electric and hybrid vehicles. The model incorporates fundamental resistive forces including rolling resistance, aerodynamic drag, gradient resistance, and acceleration resistance, each implemented as modular subsystems in Simulink. The FTP-75 drive cycle, widely recognized for emulating urban driving conditions, is used as the input speed profile to evaluate vehicle behavior under dynamic scenarios such as acceleration, deceleration, and stop-and-go traffic. Simulation outputs include time-based profiles of tractive effort, instantaneous power, and wheel torque, providing clear insights into the energy demands. Results indicate that tractive effort peaks during acceleration and uphill segments, while aerodynamic drag becomes dominant at higher speeds. Power requirements fluctuate up to approximately 70 kW, and torque values reach around 1600 Nm, consistent with medium-sized passenger vehicles. The findings confirm that the proposed framework accurately tracks the reference velocity profile and generates performance estimates. Overall, this study demonstrates the effectiveness of drive cycle-based modeling in supporting motor sizing, battery capacity planning, and control strategy development, offering a valuable foundation for both academic research and industrial vehicle design optimization.

Keywords –Vehicle Longitudinal Dynamics, Tractive Effort, Drive Cycle Simulation, Resistive Forces Modeling, MATLAB/Simulink, Power And Torque Analysis, Energy Consumption.

I. INTRODUCTION

The global shift toward sustainable mobility has intensified the need for accurate and scalable vehicle modeling techniques that support energy-efficient design and performance evaluation. As electric and hybrid vehicles become increasingly prevalent, understanding the longitudinal dynamics of road vehicles—those governing motion along the direction of travel—has become essential for optimizing propulsion systems, estimating energy consumption, and designing control strategies [1], [2]. Longitudinal dynamics encompass the interaction of tractive forces and resistive loads, including rolling resistance, aerodynamic

drag, gradient resistance, and acceleration resistance, all of which vary with driving conditions and vehicle parameters [3], [4].

Simulation-based approaches have emerged as indispensable tools in automotive engineering, enabling researchers to replicate driving scenarios in a controlled digital environment. MATLAB/Simulink, in particular, offers a robust platform for modeling vehicle subsystems and analyzing their dynamic responses under standardized drive cycles such as FTP-75, WLTC, and IDC [5], [6]. These cycles emulate urban and highway driving behaviors, allowing for detailed evaluation of vehicle performance, energy demand, and emissions. By importing time-speed profiles and integrating them with physical models, engineers can assess how vehicles respond to acceleration, deceleration, and load variations over time [7].

Recent developments in model-based design (MBD) have further enhanced the fidelity and flexibility of simulation frameworks. Modular architectures in Simulink allow for subsystem-level analysis, facilitating the isolation of key components such as propulsion units, braking systems, and energy storage modules [8]. Moreover, the inclusion of battery state-of-charge (SOC) dynamics, regenerative braking models, and torque estimation algorithms has made it possible to simulate electric and hybrid vehicles [9], [10]. These capabilities are critical for motor sizing, battery capacity planning, and control algorithm validation.

This study presents a comprehensive longitudinal vehicle dynamics model developed in MATLAB/Simulink, designed to quantify tractive effort, power demand, and wheel torque. The wheel torque represents the torque required at the wheels to overcome resistive forces and achieve the desired acceleration. The model incorporates physical equations for resistive force calculations and uses the FTP-75 drive cycle as a reference input to simulate urban driving behavior. Simulation outputs are analyzed through scope graphs, providing time-based insights into force fluctuations, energy consumption, and drivetrain performance. The proposed framework serves as a foundational tool for both academic research and industrial applications in electric and hybrid vehicle development.

II. MATERIALS AND METHOD

This study employs a modular simulation framework developed in MATLAB/Simulink to analyze the longitudinal dynamics of a passenger vehicle under standardized drive cycle conditions. The model is structured around key subsystems that calculate resistive forces, tractive effort, power demand, and wheel torque. Each subsystem is built using physical equations derived from established vehicle dynamics principles.

Resistive forces are modeled individually to reflect driving conditions. Rolling resistance is calculated as a function of vehicle mass, gravitational acceleration, road slope, and a rolling resistance coefficient, which varies depending on surface type. Aerodynamic drag is determined using air density, frontal area, drag coefficient, and vehicle speed, with the force increasing quadratically with velocity. Gradient resistance is computed based on the road incline angle and vehicle weight, while acceleration resistance accounts for the inertial effects of the vehicle's mass and rotating components during speed changes.

The simulation integrates the FTP-75 drive cycle as a time-speed input profile, representing urban driving behavior with frequent acceleration and deceleration phases. This profile drives the dynamic response of the model, enabling time-based tracking of velocity, tractive force, power requirement, and wheel torque. The wheel radius is used to convert linear force into rotational torque.

Tractive (F_t) is the force that propels the vehicle forward (see Figure 1). It is generated at the point where the tires come into contact with the road surface. It comes from the power unit (engine) and is transmitted to the wheels via the transmission components (gearbox, differential). Resistive forces are forces that slow down or stop the vehicle's movement.

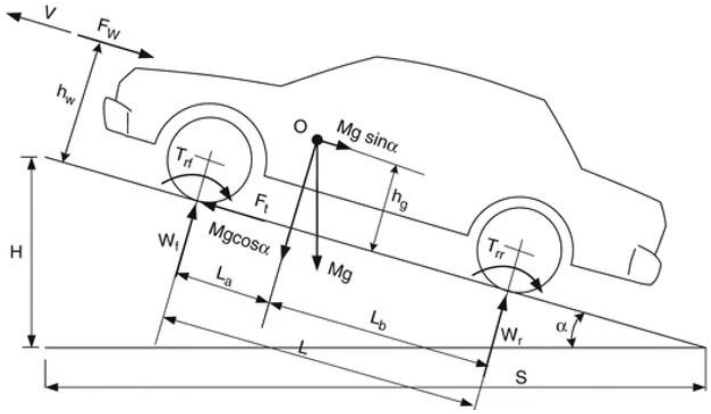

Fig. 1 The forces acting on the vehicle in longitudinal motion, including tractive and resistive forces

Rolling resistance is the energy loss caused by internal friction (hysteresis) in the tire material when the tires roll on the road surface. This resistance makes it harder for the vehicle to move forward and causes it to consume more energy. Equation for rolling resistance is given in Equation 1.

$$F_{rr} = M * g * f_r * \cos(\alpha) \quad (1)$$

In the formula M is the mass of the vehicle (kg), g is the acceleration due to gravity (9.81 m/s²), f_r is the rolling resistance coefficient, and cos(α) is the angle of inclination of the road in radians. This formula shows how rolling resistance is calculated on an inclined surface. Rolling resistance coefficients for different surfaces are shown in Table 1.

Table 1. Rolling resistance coefficients for different road surfaces

Road Condition	Coefficient (f_r)
Smooth asphalt road	0.010
Concrete road	0.015
Gravel road	0.020
Dirt road	0.030
Poor surface (e.g. mud)	0.050
Wheel on railway track	0.001

These coefficients show how much rolling resistance varies on different surfaces. For example, resistance is very low on very smooth surfaces such as railway tracks, but quite high on muddy or rough roads. Figure 2 shows how rolling resistance is implemented in Simulink.

Aerodynamic drag is the force created by air hitting the front surface of a vehicle as it moves. This force makes it harder for the vehicle to move forward and requires the engine to produce more power. Equation for aerodynamic drag is given in Equation 2.

$$F_{ad} = 0.5 * \rho * A_f * C_d * V^2 \quad (2)$$

In the formula ρ is the density of air (kg/m³), A_f is the front surface area of the vehicle (m²), Cd is the drag coefficient (depending on the shape of the vehicle), and V is the speed of the vehicle (m/s). This formula shows that aerodynamic drag force increases with the square of the speed. In other words, if the speed doubles, the drag force quadruples. Cd coefficients by vehicle type are given in Table 2.

Table 2. C_d coefficient by vehicle type

Vehicle Type	C_d (Drag Coefficient)
Motorcycle (driverless)	0.50
Motorcycle (with driver)	0.90
Convertible	0.60
Bus	0.65
Truck	0.60
Truck with trailer	0.80
Articulated vehicle (truck)	0.60

These coefficients vary depending on the vehicle's shape and aerodynamic structure. Vehicles with more aerodynamic designs have lower C_d values. And the corresponding Simulink subsystem block diagram is shown in Figure 3.

Gradient resistance When a vehicle climbs uphill, a component of its weight acts in the opposite direction to the direction of movement, creating resistance. When the vehicle descends downhill, this component facilitates movement, contributing to the vehicle's forward motion. Equation for gradient resistance is given in Equation 3.

$$F_{gr} = M * g * \sin(\alpha) \tag{3}$$

In this formula, M is the mass of the vehicle (kg), g is the acceleration due to gravity (9.81 m/s²), and α is the angle of inclination of the road in radians. This formula calculates the gravitational force experienced by the vehicle based on the angle of inclination. And the corresponding Simulink subsystem block diagram is shown in Figure 4.

Acceleration resistance: When a vehicle is travelling at a constant speed, it encounters only constant resistance (rolling, air resistance, etc.). However, during acceleration or braking, additional resistance is generated due to the vehicle's mass and the inertia of its rotating parts. This resistance requires the engine to produce more power. Equation for acceleration resistance is given in Equation 4.

$$F_a = \text{lambda} * M * \frac{dV}{dt} \tag{4}$$

In this formula, λ is a constant representing the inertia of rotating parts (Rotational Inertia Constant), M is the mass of the vehicle (kg), and dV/dt is the change in speed over time, i.e. acceleration (m/s²). This formula shows that acceleration resistance depends on both the mass of the vehicle and the amount of acceleration. And the corresponding Simulink subsystem block diagram is shown in Figure 5.

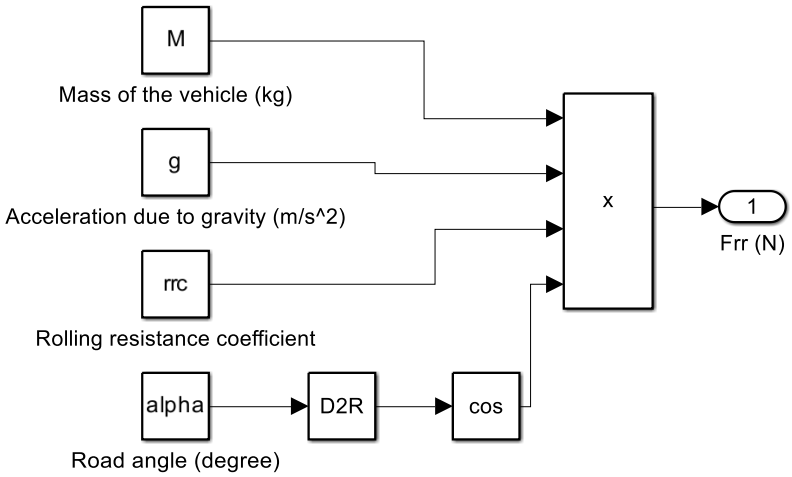

Fig. 2 Simulink subsystem block diagram representing the calculation of rolling resistance force.

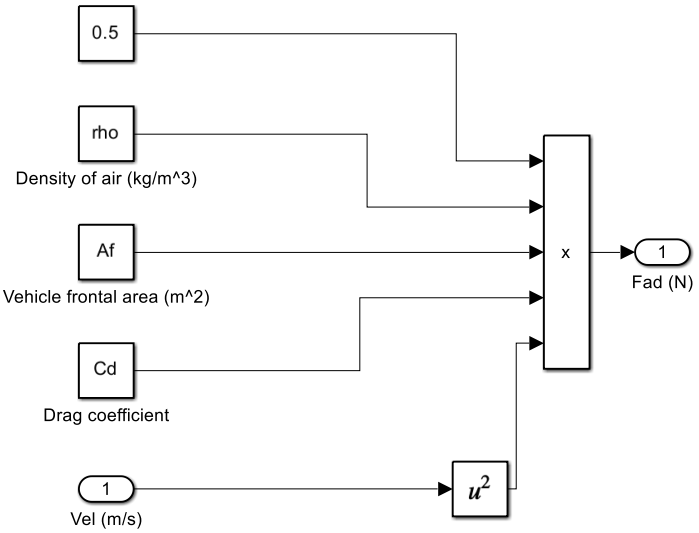

Fig. 3 Simulink subsystem block diagram illustrating the aerodynamic drag force calculation

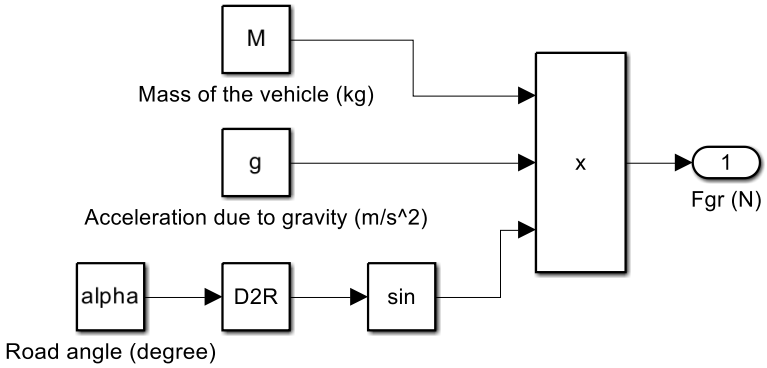

Fig. 4 Simulink subsystem block diagram showing the gradient resistance force modeling

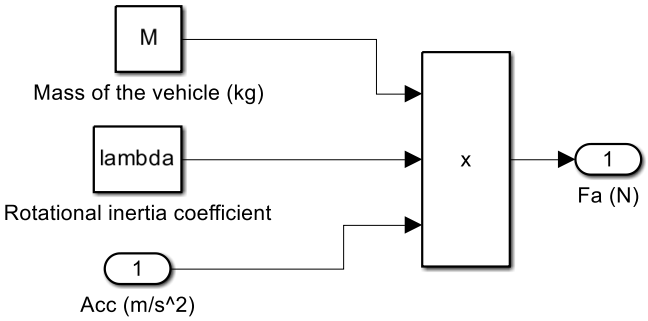

Fig. 5 Simulink subsystem block diagram for acceleration resistance force calculation

In vehicle dynamics modelling, total tractive effort (TTE), power and torque calculations are critical in determining the physical quantities required for a vehicle to move.

The wheel radius is necessary to establish the relationship between vehicle speed and wheel rotation speed. When engine torque is transmitted to the wheel, it is converted into force through the radius. In simulations, the correct wheel radius is essential for obtaining realistic results. The codes on the wheel, for example: 225/55R17, indicate 225 tire width (mm), 55 aspect ratio, i.e. the ratio of sidewall height to width (60%), R radial structure (tire type) and 17 rim diameters (inches). For 225/55 R17, r = 0.5·(0.225·0.55·2 + 0.4318) = 0.339 m.

Total Tractive Force (Ft) is expressed as follows: $F_t=F_{rr}+F_{ad}+F_{gr}+F_a$. Here, F_{rr} is rolling resistance, Fad is aerodynamic drag, F_{gr} is gradient resistance, and Fa is acceleration resistance. This formula gives the total force required for the vehicle to move forward.

Total Power Required (P_{req}) is expressed as follows: $P_{req}=F_t \cdot V$. Here V is the vehicle speed (m/s). The result is obtained as the power requirement in watts. This formula calculates the power that the engine must produce for the vehicle to move forward at a certain speed.

Torque on Wheels (τ) is expressed as: $\tau=F_t \cdot R_{wheel}$. Here, Ft is the tractive force, and R_{wheel} is the wheel radius (meters). The result is the torque obtained in Newton-meters (Nm). This formula provides the rotational force (torque) that the engine must transmit to the wheel.

These calculations are used to model vehicle performance, particularly in simulation environments such as Simulink. Accurate calculation of these three quantities is necessary to create a realistic driving profile.

All vehicle and environmental parameters—such as mass (1600 kg), frontal area (2.3 m²), drag coefficient (0.3), rolling resistance coefficient (0.01), and air density (1.23 kg/m³)—are kept constant across simulations to ensure consistency. The simulation runs over the full duration of the drive cycle, and outputs are logged for post-processing and graphical analysis. Scope graphs are used to visualize the variation of tractive effort, power, and torque over time, providing insight into the vehicle's performance under dynamic load conditions. Table 3 summarizes the key vehicle specifications and environmental conditions used in the simulations. Equivalent mass factor λ = 1.04–1.08 for front-wheel-drive passenger cars [11]. The angle of inclination (α) is specified in radians in the equations but is given as 7 degrees in Table 3. This is converted in Simulink.

Table 3. Parameters used in simulation

Parameter	Value	Description
Vehicle Mass	1600 kg	Total weight of the vehicle
Gravitational Acceleration	9.81 m/s²	Physical constant
Rolling Resistance Coeff.	0.01	For smooth surfaces such as asphalt
Slope Angle (Degrees)	7	Slope of the road
Air Density	1.23 kg/m³	Standard value at sea level
Vehicle Front Area	2.3 m²	For aerodynamic calculations
Aerodynamic Drag Coefficient (C_d)	0.3	Depends on the vehicle shape
Rotational Inertia Constant (λ)	1.05	Used in acceleration resistance calculations
Tire Radius (m)	0.339	Value obtained from previous calculations

A drive cycle is a graphical data set that shows the speed changes of a vehicle over a specific period of time. It is used to simulate real road conditions in a laboratory environment. Various drive cycles have been developed by different countries and institutions. It is used in areas such as testing vehicle control systems, energy consumption and efficiency analysis, battery life and range estimation (especially for electric vehicles), and performance comparison in different scenarios. For example, UDDS (Urban Dynamometer Driving Schedule) simulates city driving with low speeds and frequent stops and starts. FTP72 (Federal Test Procedure) is a test cycle used in the United States. It includes both urban and highway conditions. These graphs can be directly used in simulation environments such as Simulink to test vehicle behavior.

Figure 6 illustrates the overall Simulink model architecture, highlighting the flow of signals between subsystems such as the drive cycle input, resistive force block, tractive effort calculator, and energy analysis module. This visual representation aids in understanding the modular structure and data flow within the simulation.

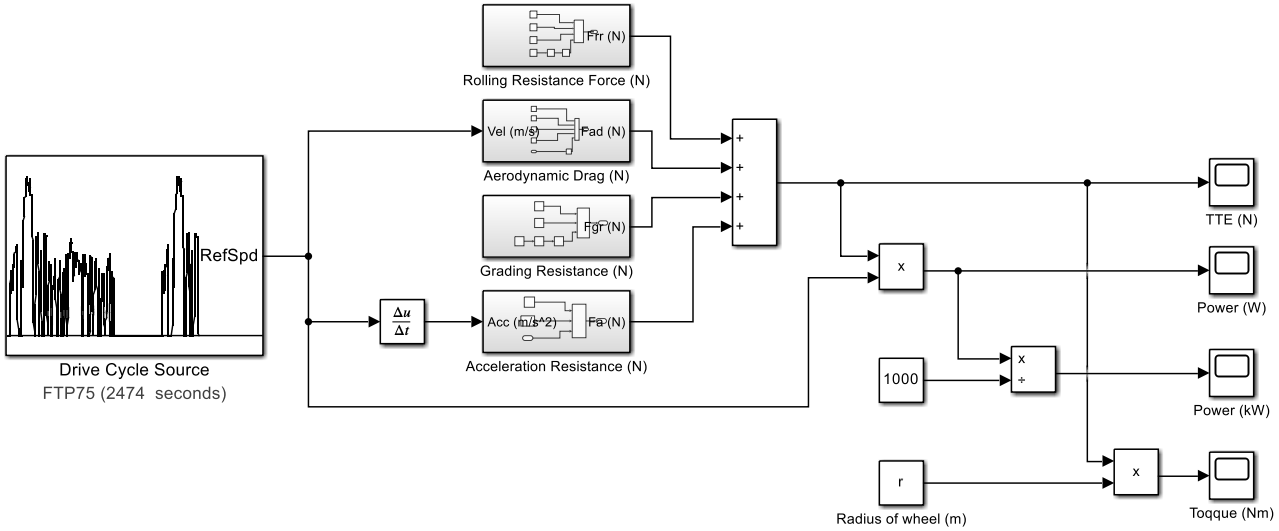

Fig. 6 Overall Simulink model architecture depicting subsystem interconnections and signal flow for longitudinal vehicle dynamics simulation

The simulation is executed over the full duration of each drive cycle, and outputs are logged for post-processing. Power and torque demands are calculated at each time step, and cumulative energy consumption is derived by integrating power over time. The model is validated by comparing simulated velocity profiles against the reference drive cycle inputs, ensuring accurate tracking and dynamic response.

III. RESULTS

This Simulink diagram performs vehicle dynamics modelling based on a driving cycle. Using a standard driving cycle called FTP-75 (see Figure 7), the forces, power and torque requirements encountered by the vehicle over time are calculated.

The basic structure of the simulation can be explained as follows: The speed-time profile provided as input by the Drive Cycle Source (FTP-75 – 2474 seconds) determines how the vehicle accelerates during the simulation. Resistance forces (Force in Newton) include F_{rr} rolling resistance, Fad aerodynamic drag, F_{gr} gradient resistance, and Fa acceleration resistance. These four forces are calculated based on the speed data that changes over time.

TTE is a force output that changes over time. The sum of all resistance forces is calculated as: $TTE(t) = F_{rr}(t) + F_{ad}(t) + F_{gr}(t) + F_a(t)$. Power calculation is expressed by the formula: Power = TTE × speed (m/s). It can be calculated in kW by dividing 1000. For torque calculation, the formula Torque = TTE × wheel radius is used to obtain the wheel torque that changes over time.

As simulation outputs, TTE (N) represents the total force required by the vehicle at each time point, Power (kW) represents the power that the vehicle's engine must produce, and Torque (Nm) represents the rotational force generated at the wheels.

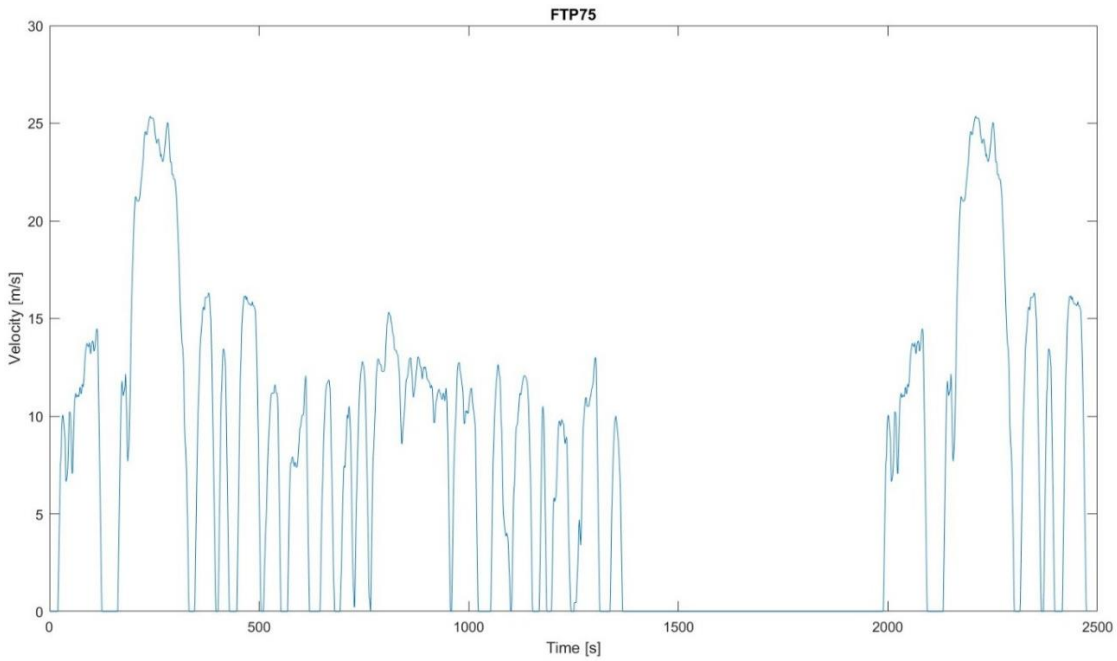

Fig. 7. FTP-75 drive cycle velocity-time profile used as input speed data for the simulation

Figure 8 illustrates the variation of TTE throughout the FTP-75 drive cycle. The results show that the required tractive force fluctuates significantly, with peaks reaching nearly 5000 N during acceleration phases and uphill segments. These peak values correspond to transient driving conditions where additional power is demanded to overcome inertial and gradient resistances. Conversely, during cruising or idling periods, the tractive force remains close to zero, reflecting steady-state operation and minimal energy demand. The observed fluctuations confirm the dynamic nature of urban driving, where frequent stop-and-go conditions impose substantial variability on drivetrain requirements. Such insights are particularly important for evaluating motor sizing and energy management strategies in electric and hybrid vehicles, as undersized propulsion units may fail to meet peak load demands while oversized systems could reduce overall efficiency.

Figure 9 presents the instantaneous power demand of the vehicle over the FTP-75 drive cycle. The results indicate that power requirements fluctuate between 0 and approximately 70 kW, with sharp peaks during rapid acceleration and uphill driving phases. These peak values represent critical load conditions that directly influence motor selection and battery discharge characteristics. In contrast, during steady cruising and deceleration phases, power demand drops considerably, even approaching zero when the vehicle is idling. The dual-phase structure of the cycle—initial urban stop-and-go followed by higher-speed operation—produces distinct power demand patterns, with the latter phase requiring sustained energy delivery at higher levels. Such variability highlights the importance of capturing transient behaviors in vehicle simulations, as average power alone does not fully represent real driving requirements. These findings underscore the necessity of ensuring that propulsion systems are capable of handling both transient peak loads and sustained operating conditions without compromising efficiency or system reliability.

Figure 10 shows the wheel torque profile generated by the simulation under the FTP-75 drive cycle. The torque demand fluctuates between 0 and approximately 1600 Nm, with pronounced peaks during acceleration and uphill phases. These peaks highlight the rotational effort required to overcome both inertial and gradient resistances, emphasizing the need for sufficient drivetrain capacity during transient load conditions. In contrast, during steady cruising, torque levels stabilize at lower values, reflecting the reduced force requirements of constant-speed operation. The presence of distinct high-torque events underlines the importance of accurately modeling transient dynamics, as average values may underestimate the true mechanical demands placed on the system. For electric vehicles in particular, these results have direct implications for motor sizing, gear ratio selection, and the design of regenerative braking strategies. The torque profile confirms that urban driving conditions impose highly variable load patterns, which must be

accounted for in both component design and control strategy development to ensure performance and efficiency.

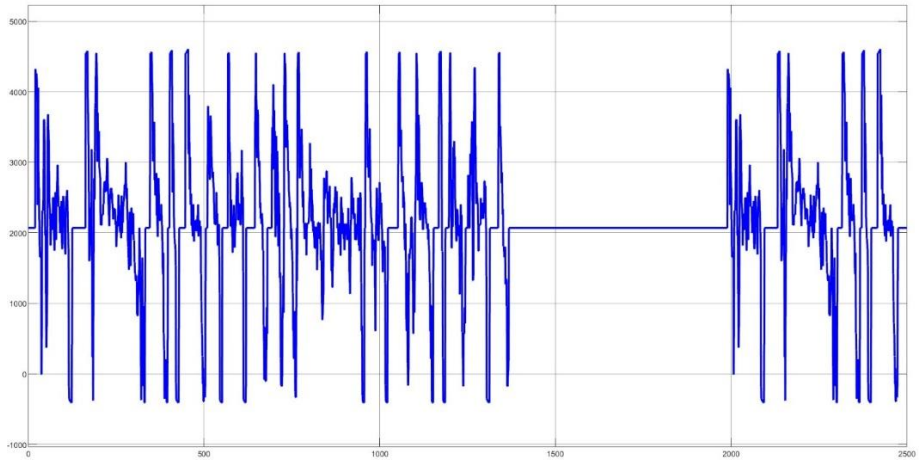

Fig. 8 Time-domain variation of TTE during the FTP-75 drive cycle showing fluctuations in driving conditions

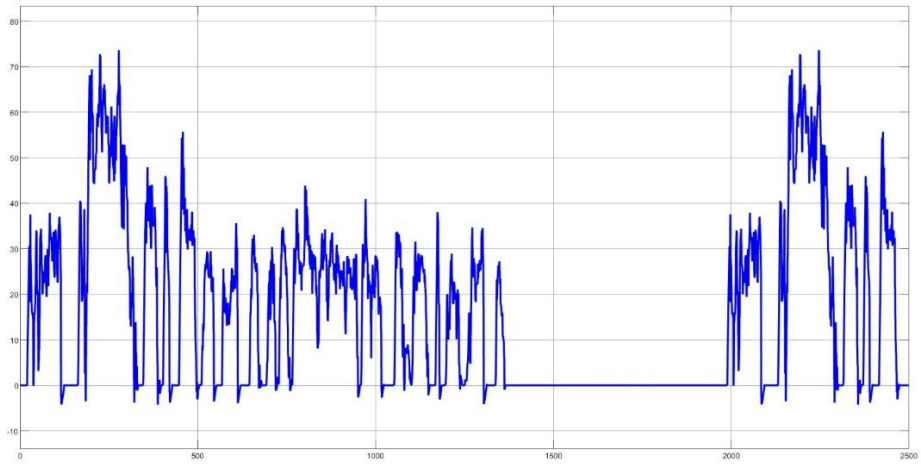

Fig. 9 Instantaneous power demand profile of the vehicle over the FTP-75 drive cycle indicating peak power requirements

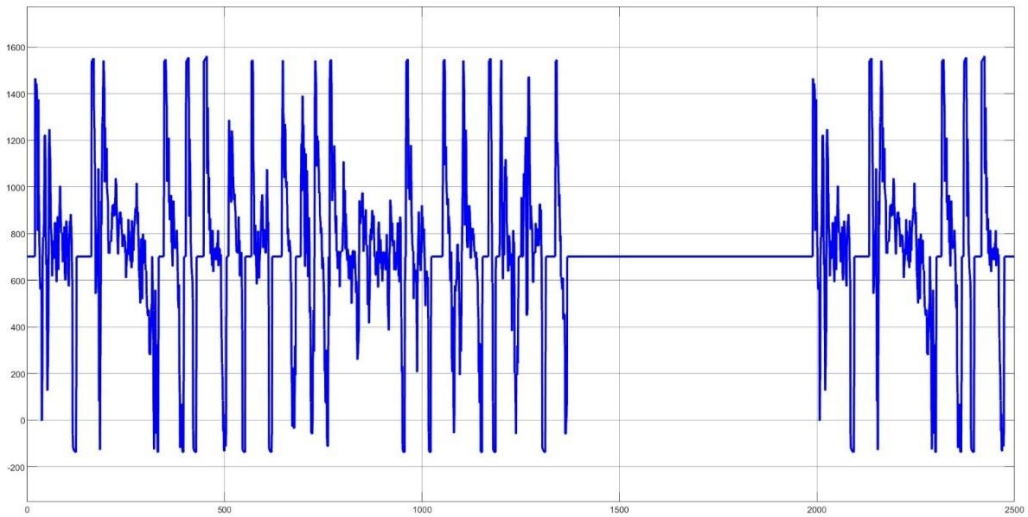

Fig. 10 Wheel torque variation profile generated from the longitudinal dynamics simulation under the FTP-75 drive cycle

IV. DISCUSSION

The simulation results confirm the robustness and applicability of the proposed MATLAB/Simulink framework for modeling longitudinal vehicle dynamics. By integrating the FTP-75 drive cycle as a reference input, the model successfully replicates the time-dependent variations in tractive effort, power demand, and wheel torque. These outputs reflect the dynamic characteristics of urban driving, where frequent acceleration, deceleration, and idling phases impose fluctuating energy demands. The scope plots clearly identify operational zones, with peak requirements occurring during rapid acceleration and uphill segments, while steady-state cruising phases exhibit more stable values [12].

A closer examination of resistive forces highlights their distinct contributions throughout the drive cycle. Rolling resistance remains nearly constant, determined mainly by vehicle mass and surface conditions, whereas aerodynamic drag exhibits a quadratic relationship with velocity, dominating at higher speeds. Gradient resistance varies with road slope and contributes significantly on inclines, while acceleration resistance emerges as a critical factor during transient maneuvers. These observations align with established findings in vehicle dynamics research, which emphasize accurate decomposition of resistive forces in performance analysis [13], [14].

The power and torque profiles derived from the model provide valuable insight into drivetrain behavior and energy consumption patterns. Peak power demands coincide with periods of high tractive effort, underscoring the importance of matching electric motor capabilities with dynamic load requirements. Torque fluctuations reveal the rotational demands imposed at the wheels, which are directly influenced by resistive forces and speed variations. Such insights are particularly relevant to electric vehicle development, where accurate estimation of motor size, battery capacity, and regenerative braking strategies plays a critical role in system optimization [15].

Moreover, the modular architecture of the Simulink model enhances its adaptability for both academic and industrial applications. Individual subsystems can be modified to include advanced control algorithms, alternative energy storage technologies, or real-time feedback mechanisms. This flexibility supports model-based design (MBD) approaches and accelerates prototyping of advanced electric and hybrid vehicle powertrains [16]. Overall, the proposed framework demonstrates significant potential as a scalable and reliable tool for evaluating vehicle performance, contributing both to sustainable mobility research and to engineering practice.

V. CONCLUSION

This study has developed and demonstrated a MATLAB/Simulink-based framework for modeling the longitudinal dynamics of passenger vehicles using standardized drive cycle inputs. The use of the FTP-75 drive cycle allowed for a time-domain evaluation of tractive effort, power demand, and wheel torque, providing meaningful insights into the dynamic requirements of propulsion systems.

The results confirmed that the model accurately tracks the reference velocity profile. These outputs highlight critical phases such as rapid acceleration, hill climbing, and cruising, thereby offering a reliable basis for evaluating drivetrain performance and energy consumption. The findings demonstrate that the proposed framework can serve as a practical tool for supporting the design of electric and hybrid vehicles, particularly in motor sizing, battery capacity estimation, and the development of energy management strategies.

In addition to its current scope, the modular architecture of the model ensures adaptability for future applications. Extensions could include the integration of regenerative braking, state-of-charge (SOC) dynamics, and alternative drive cycles such as WLTC for a broader range of operating conditions. By providing a balance between physical accuracy and modeling flexibility, this framework establishes a foundation for both academic research and industrial applications in sustainable vehicle design and optimization.

REFERENCES

[1] B. Urazel and K. Keskin, "Electric Drive Vehicle Model and Simulation with MATLAB," *Iğdır Üniversitesi Fen Bilim. Enstitüsü Derg.*, vol. 10, no. 4, pp. 2461–2473, Dec. 2020, doi: 10.21597/jist.705205.

[2] M. Ehsani, Y. Gao, and A. Emadi, *Modern Electric, Hybrid Electric, and Fuel Cell Vehicles*. CRC Press, 2017. doi: 10.1201/9781420054002.

[3] A. L. G. Sciarretta, "Control of hybrid electric vehicles," *IEEE Control Syst.*, vol. 27, no. 2, pp. 60–70, Apr. 2007, doi: 10.1109/MCS.2007.338280.

[4] S. F. Tie and C. W. Tan, "A review of energy sources and energy management system in electric vehicles," *Renew. Sustain. Energy Rev.*, vol. 20, pp. 82–102, Apr. 2013, doi: 10.1016/j.rser.2012.11.077.

[5] V. Krithika and C. Subramani, "A comprehensive review on choice of hybrid vehicles and power converters, control strategies for hybrid electric vehicles," *Int. J. Energy Res.*, vol. 42, no. 5, pp. 1789–1812, Apr. 2018, doi: 10.1002/er.3952.

[6] N. Guler, Z. M. Ismail, Z. Ben Hazem, and N. Naik, "Adaptive Fuzzy Logic Controller-Based Intelligent Energy Management System Scheme for Hybrid Electric Vehicles," *IEEE Access*, vol. 12, pp. 173441–173454, 2024, doi: 10.1109/ACCESS.2024.3496897.

[7] A. Khaligh and Zhihao Li, "Battery, Ultracapacitor, Fuel Cell, and Hybrid Energy Storage Systems for Electric, Hybrid Electric, Fuel Cell, and Plug-In Hybrid Electric Vehicles: State of the Art," *IEEE Trans. Veh. Technol.*, vol. 59, no. 6, pp. 2806–2814, Jul. 2010, doi: 10.1109/TVT.2010.2047877.

[8] M. Ceraolo, "New dynamical models of lead-acid batteries," *IEEE Trans. Power Syst.*, vol. 15, no. 4, pp. 1184–1190, 2000, doi: 10.1109/59.898088.

[9] J. Larminie and J. Lowry, *Electric vehicle technology explained*. John Wiley & Sons, 2012.

[10] A. Emadi, K. Rajashekara, S. S. Williamson, and S. M. Lukic, "Topological Overview of Hybrid Electric and Fuel Cell Vehicular Power System Architectures and Configurations," *IEEE Trans. Veh. Technol.*, vol. 54, no. 3, pp. 763–770, May 2005, doi: 10.1109/TVT.2005.847445.

[11] G. Genta and L. Morello, "Multibody Modelling," in *The Automotive Chassis: Volume 2: System Design*, Springer, 2019, pp. 627–694.

[12] M. B. Camara, H. Gualous, F. Gustin, and A. Berthon, "Design and New Control of DC/DC Converters to Share Energy Between Supercapacitors and Batteries in Hybrid Vehicles," *IEEE Trans. Veh. Technol.*, vol. 57, no. 5, pp. 2721–2735, Sep. 2008, doi: 10.1109/TVT.2008.915491.

[13] S. M. Lukic, Jian Cao, R. C. Bansal, F. Rodriguez, and A. Emadi, "Energy Storage Systems for Automotive Applications," *IEEE Trans. Ind. Electron.*, vol. 55, no. 6, pp. 2258–2267, Jun. 2008, doi: 10.1109/TIE.2008.918390.

[14] X. Zhao, J. Zhang, and J. Tang, "Optimal control for shift mechanism of a planetary two-speed transmission for electric vehicles," *Int. J. Electr. Hybrid Veh.*, vol. 14, no. 3, p. 231, 2022, doi: 10.1504/IJEHV.2022.125585.

[15] S. De Pinto *et al.*, "On the Comparison of 2- and 4-Wheel-Drive Electric Vehicle Layouts with Central Motors and Single- and 2-Speed Transmission Systems," *Energies*, vol. 13, no. 13, p. 3328, Jun. 2020, doi: 10.3390/en13133328.

[16] B. Bairwa, S. B, C. Pratiksha, and S. A, "Modeling and Simulation of Electric Vehicle Powertrain for Dynamic Performance Evaluation," in *2023 International Conference on Distributed Computing and Electrical Circuits and Electronics (ICDCECE)*, IEEE, Apr. 2023, pp. 1–7. doi: 10.1109/ICDCECE57866.2023.10150956.